Research Article

A novel gain-of-function Na$_v$1.7 mutation in a carbamazepine-responsive patient with adult-onset painful peripheral neuropathy

Talia Adi[1,2] , Mark Estacion[1,2], Betsy R Schulman[1,2],
Steven Vernino[3], Sulayman D Dib-Hajj[1,2], and
Stephen G Waxman[1,2]

Abstract

Voltage-gated sodium channel Na$_v$1.7 is a threshold channel in peripheral dorsal root ganglion (DRG), trigeminal ganglion, and sympathetic ganglion neurons. Gain-of-function mutations in Na$_v$1.7 have been shown to increase excitability in DRG neurons and have been linked to rare Mendelian and more common pain disorders. Discovery of Na$_v$1.7 variants in patients with pain disorders may expand the spectrum of painful peripheral neuropathies associated with a well-defined molecular target, thereby providing a basis for more targeted approaches for treatment. We screened the genome of a patient with adult-onset painful peripheral neuropathy characterized by severe burning pain and report here the new Na$_v$1.7-V810M variant. Voltage-clamp recordings were used to assess the effects of the mutation on biophysical properties of Na$_v$1.7 and the response of the mutant channel to treatment with carbamazepine (CBZ), and multi-electrode array (MEA) recordings were used to assess the effects of the mutation on the excitability of neonatal rat pup DRG neurons. The V810M variant increases current density, shifts activation in a hyperpolarizing direction, and slows kinetics of deactivation, all gain-of-function attributes. We also show that DRG neurons that express the V810M variant become hyperexcitable. The patient responded to treatment with CBZ. Although CBZ did not depolarize activation of the mutant channel, it enhanced use-dependent inhibition. Our results demonstrate the presence of a novel gain-of-function variant of Na$_v$1.7 in a patient with adult-onset painful peripheral neuropathy and the responsiveness of that patient to treatment with CBZ, which is likely due to the classical mechanism of use-dependent inhibition.

Keywords

Neuropathic pain, sodium channel, Nav1.7, mutation, DRG neuron, carbamazepine

Introduction

Chronic pain is a frequent and major unmet global challenge.[1,2] Current treatments for chronic pain include sodium channel blockers, but these are often not very effective and are accompanied by side effects that limit their use even when relief is initially observed.[3] Although general guidelines have been developed, treatment remains largely dependent on a trial-and-error strategy for individual patients. A more complete understanding of underlying mechanisms for pain might lead to more informed choice of therapy.

Voltage-gated sodium channel Na$_v$1.7 has been established as a critically important "pain channel" in several

[1]Department of Neurology, Yale University School of Medicine, New Haven, CT, USA
[2]Center for Neuroscience and Regeneration Research, Veterans Affairs Medical Center, West Haven, CT, USA
[3]Department of Neurology and Neurotherapeutics, UT Southwestern Medical Center, Dallas, TX, USA

Corresponding Author:
Stephen G Waxman, Center for Neuroscience and Regeneration Research, Veterans Affairs Medical Center, 950 Campbell Avenue, Building 34, West Haven, CT 06516, USA.
Email: stephen.waxman@yale.edu

human pain disorders. $Na_v1.7$ is preferentially expressed in peripheral somatic and visceral sensory neurons within dorsal root ganglia (DRG) and in sympathetic ganglion neurons[4,5] and is characterized by a slow rate of closed-state inactivation, enabling channels to activate in response to small, slow depolarizations, thereby amplifying small stimuli.[6] Thus, $Na_v1.7$ has been considered to act as a threshold channel which can set the gain of nociceptors.[7] Dynamic clamp studies[8] and pharmacological block using $Na_v1.7$-selective blockers[9] have provided strong evidence supporting the role of $Na_v1.7$ in regulating both threshold for action potentials in rodent and human DRG sensory neurons and neurotransmitter release from peripheral and central terminals of mouse primary afferents.[9,10] Knockout of $Na_v1.7$ increases pain threshold in animal models,[10–13] further supporting the contribution of this channel to pain.

Genetic studies in humans have provided compelling evidence for the role of $Na_v1.7$ in rare Mendelian pain disorders and in more common painful peripheral neuropathy. Familial and sporadic dominant gain-of-function mutations in $Na_v1.7$ have been identified in patients with the painful disorders inherited erythromelalgia (IEM) and paroxysmal extreme pain disorder (PEPD).[4,5] Studies of more common painful peripheral neuropathy have identified gain-of-function variants in patients with idiopathic small fiber neuropathy (SFN)[14] and in patients with painful diabetic neuropathy.[15] Patients with IEM or $Na_v1.7$-related painful peripheral neuropathy experience attacks of excruciating pain, usually most intense in the distal extremities (feet and hands), which in IEM are exacerbated by mild warmth or exercise and relieved by cooling. Most patients with IEM are resistant to pharmacotherapy and do not report relief with any available agents, while patients with PEPD generally respond to treatment with carbamazepine (CBZ).[16] Although $Na_v1.7$-selective blockers have started to be tested in clinical studies,[17] they have not yet reached clinical use. However, pharmacogenomic studies have revealed a novel mode of action of CBZ which depolarizes activation of several mutant $Na_v1.7$ channels, and pain in patients with these specific $Na_v1.7$ mutations is relieved by CBZ,[18,19] suggesting that a personalized medicine approach might become available in the foreseeable future.

These studies suggest that identification of $Na_v1.7$ mutations in patients with painful peripheral neuropathy will not only lead to better understanding of pathophysiological mechanisms underlying pain in these patients but may also inform decisions about treatment. We report here the identification of a novel rare variant of $Na_v1.7$ in a patient with adult-onset pain symptoms and functional assessment of the effect of the mutation on the channel properties and on the excitability of DRG neurons that express this mutant channel. We also assessed the sensitivity of the channel to a clinically achievable concentration of CBZ in order to explore mechanistic basis for the responsiveness of the patient to CBZ.

Materials and methods

Patient enrollment and genomic analysis

The patient first presented to neurology clinic at the age of 53 with a chief complaint of episodic painful dysesthesias. The study participant signed informed consent and underwent clinical assessment which consisted of clinical history, neurological examination, imaging of the entire neuraxis, laboratory tests of blood and cerebrospinal fluid (CSF), and a complete serum paraneoplastic antibody panel (Mayo, Mayo Clinic Laboratories, Rochester, MN, USA). Cardiology evaluation revealed supraventricular tachycardia and atrial fibrillation, and an ablation procedure was performed. Treatment with flecainide caused a marked worsening of dysesthesias and was terminated, and eventually a pacemaker was placed.

Whole exome sequencing was performed at Baylor Miraca Genetics Laboratories (Houston, TX), and the variants that were detected in *SCN5A* and *SCN9A* were confirmed by Sanger sequencing. Rare variants that were present at <1% allele frequency in the Exome Variant Server (exome sequencing project [ESP], http://evs.gs. washington.edu/EVS), Exome Aggregation Consortium (ExAC, http://exac.broadinstitute.org), and 1000 Genomes (http://phase3browser.1000genomes.org) were selected for further analysis.

Plasmids and transfection of HEK293 cells

The human adult-long splice $Na_v1.7$ isoform complementary DNA (cDNA) has been previously described.[14] Briefly, the cDNA was cloned into a mammalian expression vector and converted to a tetrodotoxin-resistant phenotype by Y362S substitution ($hNa_v1.7_{R/AL}$, hereafter referred to as WT). The $hNa_v1.7_{R/AL}$-V810M missense mutation (hereafter referred to as V810M) was introduced using QuickChange XL site-directed mutagenesis (Stratagene, San Diego, CA). Human embryonic kidney 293 (HEK293) cells seeded onto 12 mm poly-D-lysine/laminin coated glass coverslips (Corning, Corning, Inc., Corning, NY, USA) were cotransfected with either WT or V810M plasmids (0.8 μg/well) and human β1 and β2 subunits (0.2 μg/well each) using Lipofectamine 2000 reagent (Invitrogen, Carlsbad, CA, USA). HEK293 cells were maintained under standard culture conditions (37°C with 5% CO_2) in Dulbecco's modified Eagle's medium (DMEM)/F12 medium

supplemented with 10% fetal bovine serum and 1% penicillin/streptomycin (hereafter referred to as DRG medium).

Voltage-clamp electrophysiology

Whole-cell voltage-clamp recordings were obtained at room temperature 24 h after transfection using an EPC-9 amplifier and PatchMaster software (HEKA Elektronik, Holliston, MA, USA). We alternated recordings from cells expressing either WT or V810M channels on the same day. Patch electrodes were pulled from fire-polished borosilicate glass capillaries (1.65/1.1 mm OD/ID; World Precision Instruments, Inc., Sarasota, FL, USA) using a P-97 puller (Sutter Instrument Company, Novato, CA, USA) and had a resistance of 0.8–1.3 MΩ when filled with intracellular solution, which contained (in mM): 140 CSF, 10 NaCl, 1.1 ethylene glycol tetraacetic acid, 10 hydroxyethyl piperazineethanesulfonic acid (HEPES) (pH 7.3 with CsOH, adjusted to 310 mOsm with dextrose). Extracellular solution contained (in mM): 140 NaCl, 3 KCl, 1 $CaCl_2$, 1 $MgCl_2$, 10 HEPES (pH 7.3 with NaOH, adjusted to 320 mOsm with dextrose). Pipette potentials were adjusted to zero prior to gigaseal formation, and no adjustments were made for liquid junction potential. Holding potential was set to –120 mV. Voltage errors were minimized using 80–90% series resistance compensation, and only cells with a voltage error < 3 mV after compensation were included for analysis. Leak currents were subtracted using the P/6 method, except during use-dependence protocols.

Recordings began following a 5-min equilibration period after establishing whole-cell configuration. To measure activation, cells were stepped from the holding potential of –120 mV to potentials ranging from –80 to +40 mV in 5 mV increments for 100 ms with 5 s between pulses. Current density was calculated by normalizing peak currents to cell capacitance. Peak inward currents obtained from activation protocols were converted to conductance values using the equation, $G = I/(V_m - E_{Na})$, where G is conductance, I is peak inward current, V_m is membrane potential used to elicit the current response, and E_{Na} is the reversal potential for sodium. Conductance data were then normalized to the maximum conductance value and fit to the Boltzmann equation,

$$G/G_{max} = 1/\left(1 + \exp\left[(V_m - V_{1/2})/k\right]\right) \qquad (1)$$

where $V_{1/2}$ is the midpoint of activation, and k is the slope factor. Kinetics of deactivation were measured using a short 0.5-ms depolarizing pulse to –10 mV followed by a 50-ms repolarizing pulse to potentials ranging from –40 to –120 mV in 5 mV increments. Tail currents were fit with a single-exponential equation,

$$I = A \times (\exp[-t/\tau]) + C \qquad (2)$$

where A is the amplitude of the fit, t is time, τ is the time constant of decay, and C is the steady-state asymptote. Steady-state fast inactivation was determined using a series of 500 ms prepulses ranging from –140 to –10 mV increasing in 10 mV increments followed by a 40-ms depolarization to –10 mV. Peak inward currents obtained from steady-state fast inactivation protocols were normalized to the maximum current amplitude and fit to the Boltzmann equation,

$$I/I_{max} = 1/\left(1 + \exp\left[(V_m - V_{1/2})/k\right]\right) \qquad (3)$$

where $V_{1/2}$ is the midpoint of fast inactivation, and k is the slope factor. Protocols to determine steady-state slow inactivation involved 30-s prepulses ranging from –130 mV to +30 mV increasing in 10 mV increments followed by a 100 ms hyperpolarization to –120 mV. Cells were then depolarized to –10 mV for 20 ms. Peak inward currents obtained from steady-state slow inactivation protocols were normalized to the maximum current amplitude and fit to the Boltzmann equation,

$$I/I_{max} = 1/\left(1 + \exp\left[(V_m - V_{1/2})/k\right]\right) \qquad (4)$$

where $V_{1/2}$ is the midpoint of slow inactivation, and k is the slope factor. To measure use-dependence, a train of thirty 20-ms pulses to –10 mV were conducted at a frequency of 20 Hz. Peak inward currents obtained from use-dependence protocols were normalized to the maximum current amplitude.

Isolation and transfection of primary DRG neurons

All animal care and experimental studies followed protocols approved by the Veterans Administration Connecticut Healthcare System Institutional Animal Care and Use Committee. Dorsal root ganglion (DRG) neurons from male and female Sprague-Dawley neonatal rat pups (P0-P5) were harvested and dissociated as previously described.[20] In brief, DRG neurons were dissociated with a 20-min incubation in 1.5 mg/mL collagenase A (Roche Diagnostics, Indianapolis, IN, USA) and 0.6 mM ethylenediaminetetraacetic acid (EDTA), followed by another 20-min incubation in 1.5 mg/mL collagenase D (Roche Diagnostics, Indianapolis, IN, USA), 0.6 mM EDTA, and 30 U/mL papain (Worthington Biochemical Corp., Lakewood, NJ, USA). Dissociated cells were then centrifuged and triturated in 0.5 mL DRG medium containing 1.5 mg/mL bovine serum albumin (low endotoxin) and 1.5 mg/mL trypsin inhibitor (Sigma-Aldrich, St. Louis, MO, USA). Finally, DRG neurons were transfected with either WT or V810M plasmids (2.5 µg)

using a Nucleofector IIS (Lonza, Basel, Switzerland) and Amaxa Basic Neuron SCN Nucleofector Kit (VSPI-1003). Transfected neurons were given 5 min at $37°C$ to recover in Ca^{2+}-free DMEM before being seeded onto 12-well multi-electrode array (MEA) plates (Axion Biosystems, Atlanta, GA) coated with poly-D-lysine (50 µg/mL)/laminin (10 µg/mL). DRG medium (1.5 mL per well) supplemented with 50 ng/mL each of mouse nerve growth factor (Alomone Labs, Jerusalem, Israel) and glial cell line-derived neurotrophic factor (PeproTech, Rocky Hill, NJ, USA) was added to cells.

MEA recording

MEA recordings were obtained as previously described.[21,22] Briefly, dissociated and transfected DRG neurons were maintained in standard culture conditions ($37°C$ with 5% CO_2) for at least three days prior to recording. Spontaneous firing activity of these neurons was assessed using a multi-well MEA system (Maestro, Axion Biosystems). A 12-well recording plate was used, with each well containing 64 low-noise individual embedded microelectrodes with integrated ground electrodes, forming an 8×8 recording grid of electrodes across a 2×2-mm area. Each electrode had a diameter of 30 µm with 200 µm center-to-center spacing between individual electrodes. For each experiment, three wells each (~ 192 available electrodes) of either WT or V810M were prepared and seeded. To minimize variation, DRG tissue from two different animals were pooled, prepared, and transfected with WT and V810M plasmids in parallel by the same investigator in each experiment. The investigator performing the MEA recordings was blinded to the identity of the channel expressed in each well until after recordings were completed. Three independent experiments were conducted. To provide environmental control during recordings, an ECmini unit was used to maintain CO_2 concentrations around MEA cultures with a low flow of premixed gas (5% CO_2, 20% O_2, balance nitrogen), and temperature was maintained at a physiological level of $37°C$. A spike detection criterion of > 6 standard deviations above background signal was used to distinguish action potentials from noise. Active electrodes were defined as registering > 1 recorded spike over a period of 200 s.

Drug studies

CBZ (Sigma-Aldrich) was dissolved in dimethyl sulfoxide (DMSO) to make a 30-mM ($1000\times$) stock solution. Working solutions were mixed fresh daily. Transfected HEK293 cells were preincubated for 30 min in standard culture conditions ($37°C$ with 5% CO_2) with either 30 µM CBZ or 0.1% DMSO vehicle in serum-free DMEM/F12 medium (Thermo Fisher, Waltham, MA)

as previously described.[18,22] CBZ or DMSO concentration was maintained in extracellular solution during recordings.

Data analysis and statistics

Voltage-clamp data were analyzed using FitMaster (HEKA Elektronik), Origin 2017 (OriginLab Corporation, Northampton, MA, USA), and GraphPad Prism 7.01 (GraphPad Software, La Jolla, CA, USA) software. MEA data were analyzed using Axion Integrated Studio AxIS2.1 (Axion Biosystems), NeuroExplorer (Nex Technologies, Colorado Springs, CO, USA), and Origin 2017 (OriginLab Corporation, Northampton, MA, USA). Unless otherwise noted, statistical significance was assessed using two-sample t test. Statistical significance for kinetics of deactivation and use-dependence data were evaluated using two-factor analysis of variance with repeated measures and Bonferroni *post hoc* test. Descriptive data are expressed as mean ± standard error. Data were considered significant at $p < 0.05$.

Results

Clinical phenotype and molecular genetics

The patient presented to neurology clinic at the age of 53 with a chief complaint of episodic painful dysesthesias. He had a history of itching paresthesias in the soles and heels beginning in his early 40s. At around age 48, without clear provocation, he developed severe pain down the left leg, cramping feeling in the left hand, and numbness/paresthesias in the left face. Magnetic resonance imaging of the head and neck were normal. Around the same time, he developed episodes of supraventricular tachycardia and atrial fibrillation and underwent an ablation procedure.

At the age of 53, the neurological symptoms worsened. The patient developed cramps in the hands and forearms and very painful burning in the feet, which then ascended to the knees and became more diffuse. The sensory disturbances affected all four limbs as well as the back, head, and face. The chest and abdomen were relatively unaffected, although he reported episodes of anal pain. Strength, vision, cognition, and bulbar function were normal. Imaging of the entire neuraxis and CSF examination were normal.

Brief trials of gabapentin, duloxetine, pregabalin, nortriptyline, and narcotics and a gluten-free diet were tried without benefit. A short empiric trial of oral corticosteroids seemed to improve his symptoms, and over the course of a year, symptoms improved markedly but did not completely resolve. Eventually, he was able to stop all symptomatic medication and returned to a high

level of function. At the age of 57, symptoms returned without clear inciting event. He experienced burning pain and paresthesia as well as chest pains and labile blood pressure. Supraventricular tachycardia and atrial fibrillation were treated with a second ablation procedure. Treatment with flecainide caused worsening of dysesthesias. Ultimately, he had pacemaker placed.

Diffuse neuropathic pain has continued in a relapsing/remitting pattern; pain attacks lasting for weeks are in some cases provoked by cold or vibratory stimulation, with improvement on warm days. Common symptoms during attacks are burning and stinging sensations in the face, buttocks, legs, and fingers. Low-dose amitriptyline and nortriptyline provided some benefit for nighttime symptoms. Mexiletine was not tolerated. At the age of 59, he started treatment with CBZ. The maximum tolerated dose of 300 mg per day significantly reduced frequency and severity of pain attacks.

Whole exome sequencing of the patient's DNA identified variants in *SCN9A*, the gene which encodes sodium channel $Na_v1.7$, and in *SCN5A*, the gene which encodes $Na_v1.5$. The patient showed heterozygous mutations in $Na_v1.7$ (c. 2428G>A) and $Na_v1.5$ (c. 1844G>A). These variants were confirmed using Sanger targeted sequencing of exons of both genes. The $Na_v1.7$ (c. 2428G>A) variant substitutes valine (V) by methionine (M) at position 810 (p. V810M). The variant allele is very rare (0.008%, ESP; 0.03%, ExAC; 0.02%, 1000 Genomes) and was classified in these databases as of unknown significance. Although V810, which is located at the C-terminal end of transmembrane segment 3 in domain II (DII/S3) in $Na_v1.7$, is shared with $Na_v1.1$ and $Na_v1.4$, the equivalent residue is methionine in $Na_v1.2$, $Na_v1.3$, and $Na_v1.6$; leucine in $Na_v1.8$; and alanine in $Na_v1.9$. However, V810 is highly conserved in orthologues of $Na_v1.7$ in mammalian species in which this channel has been identified (Figure 1). The conservation of a valine residue at this position in $Na_v1.7$ in different mammalian species suggests that its substitution may cause functional changes to the channel.

Voltage-clamp recordings of WT and V810M currents

To determine whether the V810M mutation alters voltage-dependent properties of $Na_v1.7$, HEK293 cells were transiently cotransfected with either WT or V810M channels and human β1 and β2 subunits, and voltage-clamp recordings performed 24 h after transfection. Representative whole-cell currents from WT and V810M mutant channels are shown in Figure 2(a). The average peak inward current density was significantly increased for V810M by 1.5-fold as compared to WT channels ($p = 0.03$; Table 1, Figure 2(b)).

Normalized voltage-dependence of activation curves are shown in Figure 2(c). Voltage midpoints ($V_{1/2}$) of activation were calculated from Boltzmann fits of
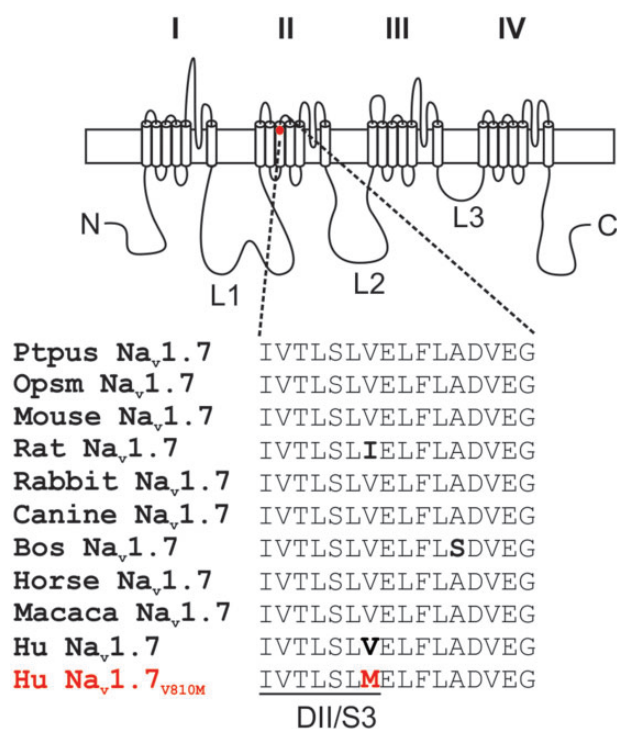

Figure 1. Sequence alignment of DII/S3-S4 of $Na_v1.7$ from mammalian species. Schematic of a voltage-gated sodium channel showing the location of V810M and sequence alignment of DII/S3-S4 from $Na_v1.7$ orthologues from mammalian species. This region is highly conserved among orthologues of $Na_v1.7$ with only two variations, an isoleucine instead of valine in the rat at the position that corresponds to V810 in human $Na_v1.7$, and an alanine to serine in the S3-4 extracellular linker in bovine $Na_v1.7$.

normalized conductance (Figure 2(d)) and show that the V810M mutation hyperpolarizes activation by 3 mV ($p = 0.04$; Table 1). The slope factor of voltage-dependent activation, which quantifies the steepness of the Boltzmann fits of normalized conductance, was unaffected by the V810M mutation (Table 1). There was no significant difference in reversal potentials between V810M and WT channels (WT: 71.2 ± 2.4 mV, $n = 18$; V810M: 68.2 ± 1.5 mV, $n = 16$). We assessed kinetics of deactivation, which represents the transition of the channel from the open state to the closed state and found that V810M currents showed significantly slowed deactivation kinetics relative to WT channels over a range of potentials from –65 to –40 mV ($p = 0.0005$; Bonferroni comparisons: –65 mV, $p = 0.02$; –60 mV, $p = 0.004$; –55 mV, $p < 0.0001$; –50 mV, $p < 0.0001$; –45 mV, $p < 0.0001$; –40 mV, $p < 0.0001$; Table 1, Figure 2(e)). The increase in peak current density, a 3-mV hyperpolarized shift in activation, and slowed deactivation kinetics of V810M all represent gain-of-function changes of the mutant channel.

V810M did not alter voltage-dependence of steady-state fast inactivation (Table 1, Figure 3(a)) or steady-state slow
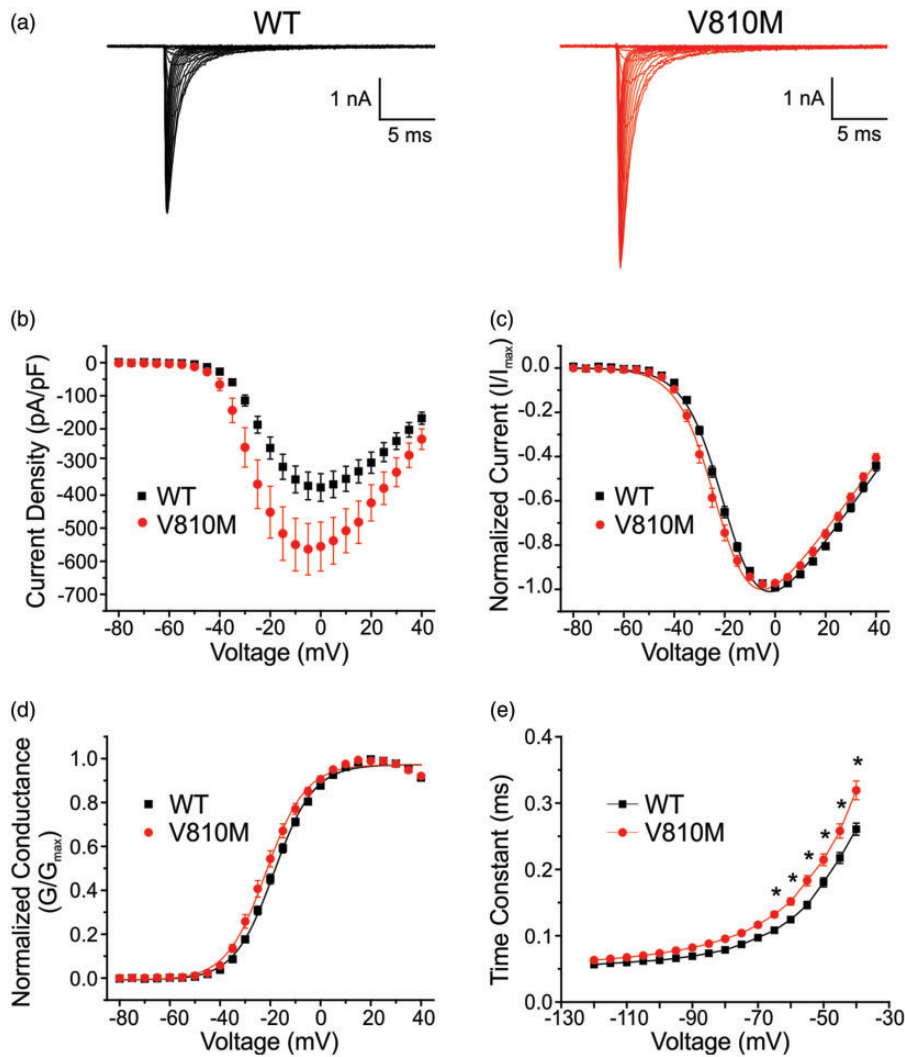
Figure 2. V810M increases peak current, hyperpolarizes voltage-dependent activation, and delays deactivation of Na$_v$1.7.
(a) Representative whole-cell current traces from HEK293 cells transiently transfected with WT (black) or V810M (red) channels. Cells were held at −120 mV and stepped to potentials ranging from −80 to +40 mV in 5 mV increments for 100 ms with 5 s between pulses. (b) Current density for WT (black squares, $n = 18$) and V810M (red circles, $n = 16$) channels showing a significant increase in peak current density for V810M. Current density was calculated by normalizing peak currents to cell capacitance. (c) Normalized peak current-voltage relationship for activation of WT (black squares, $n = 18$) and V810M (red circles, $n = 16$) channels showing a significant hyperpolarized shift in activation of V810M. (d) Voltage-dependent activation of WT (black squares, $n = 18$) and V810M (red circles, $n = 16$) channels showing a small but significant hyperpolarized shift in activation of V810M. Conductance curves were normalized to the maximum conductance value and fit to a Boltzmann equation. (e) Deactivation time constants for WT (black squares, $n = 17$) and V810M (red circles, $n = 11$) channels showing significantly slowed kinetics of deactivation for V810M over a voltage range of −65 to −40 mV. Data are expressed as means ± SEM.

Table 1. Biophysical properties of WT and V810M channels.

Na$_v$1.7	Current density		Activation (mV)			Steady-state fast inactivation (mV)			Steady-state slow inactivation (mV)			Deactivation (ms)	
	pA/pF	n	$V_{1/2}$	k	n	$V_{1/2}$	k	n	$V_{1/2}$	k	n	−40 mV	n
WT	380.1 ± 42.2	18	−18.5 ± 0.7	7.7 ± 0.1	18	−83.7 ± 1.4	6.7 ± 0.2	18	−72.2 ± 1.7	14.0 ± 0.6	8	0.26 ± 0.01	17
V810M	577.6 ± 80.3*	16	−21.5 ± 1.2*	7.4 ± 0.3	16	−85.5 ± 1.2	6.7 ± 0.2	17	−69.8 ± 1.7	14.5 ± 0.6	7	0.32 ± 0.01**	11

*$p < 0.05$, **$p < 0.0001$ significantly different from WT; n represents the number of cells from which recordings were acquired.
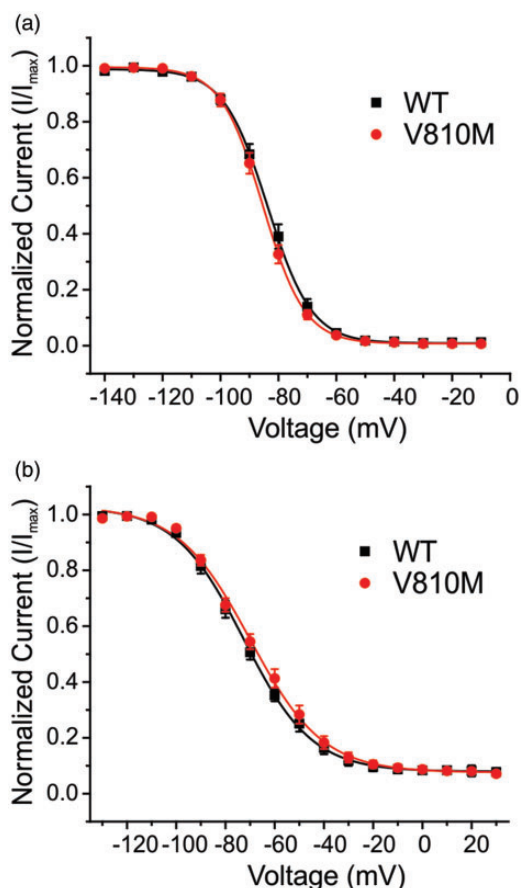
(a)

(b)

Figure 3. V810M has no effect on inactivation of Na$_v$1.7. (a) Steady-state fast inactivation of WT (black squares, $n = 18$) and V810M (red circles, $n = 17$) channels. Currents were normalized to maximum current amplitude and fit to a Boltzmann equation. (b) Steady-state slow inactivation of WT (black squares, $n = 8$) and V810M (red circles, $n = 7$) channels. Currents were normalized to maximum current amplitude and fit to a Boltzmann equation. Data are expressed as means ± SEM.

inactivation (Table 1, Figure 3(b)). Furthermore, the mutation had no effect on use-dependent inhibition at 20 Hz (ratio of peak current of the 30th pulse normalized to peak current of the first pulse: WT: 76.5 ± 1.6%, $n = 16$; V810M: 73.1 ± 2.1%, $n = 16$).

MEA recordings of WT and V810M spontaneous firing

The increase in current density and the gain-of-function changes to voltage-dependent properties of V810M suggest that this mutation may alter excitability in DRG neurons. To assess the effects of V810M on excitability of DRG neurons, we used MEA recording, which allows for a high-throughput, noninvasive approach for recording from intact neurons. Recordings were performed at the physiological core body temperature of 37°C and revealed significant differences between DRG neurons
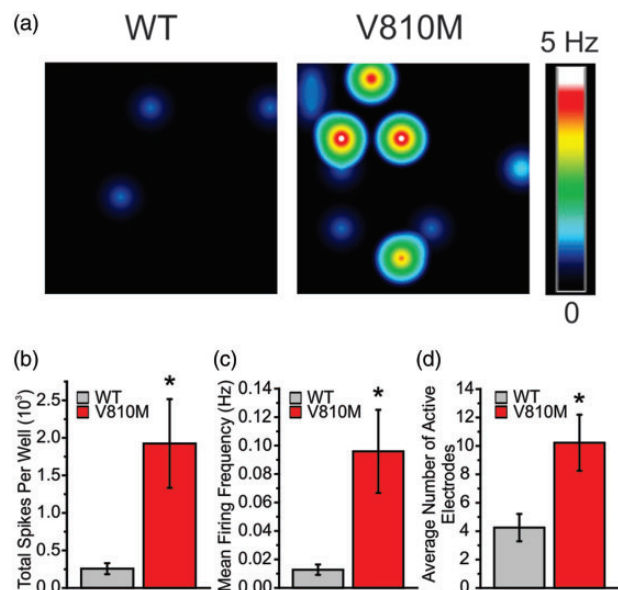

Figure 4. V810M increases firing of DRG neurons at 37°C. (a) Representative heatmaps of MEA recordings of DRG neurons expressing WT or V810M channels at 37°C. (b) Total spikes per well from DRG neurons expressing WT (gray fill, $n = 8$ wells from 3 experiments, 6 rats) and V810M (red fill, $n = 9$ experiments, 6 rats) channels, showing a significant increase in total spikes by V810M-expressing neurons. (c) Mean firing frequency (Hz) from DRG neurons expressing WT (gray fill, $n = 8$ wells from 3 experiments, 6 rats) and V810M (red fill, $n = 9$ wells from 3 experiments, 6 rats) channels, showing a significant increase in mean firing frequency by V810M-expressing neurons. (d) Average number of active electrodes from DRG sensory neurons expressing WT (gray fill, $n = 8$ wells from 3 experiments, 6 rats) and V810M (red fill, $n = 9$ wells from 3 experiments, 6 rats) channels, showing a significant increase in average number of active electrodes by V810M-expressing neurons.

expressing WT and V810M across multiple metrics of excitability, including total number of spikes per well (WT: 256.9 ± 72.9, $n = 8$ wells from 3 experiments, 6 rats; V810M: 1924.9 ± 590.8, $n = 9$ wells from 3 experiments, 6 rats; $p = 0.02$); mean firing frequency (WT: 0.013 ± 0.004 Hz, $n = 8$ wells from 3 experiments, 6 rats; V810M: 0.096 ± 0.029 Hz, $n = 9$ wells from 3 experiments, 6 rats; $p = 0.02$); and number of active electrodes per well (WT: 4.3 ± 1.0, $n = 8$ wells from 3 experiments, 6 rats; V810M: 10.2 ± 2.0, $n = 9$ wells from 3 experiments, 6 rats; $p = 0.02$; Figure 4).

Effects of CBZ on voltage-dependent properties of V810M

In an attempt to explain the mechanistic basis for CBZ-responsiveness of the patient, we performed voltage-clamp experiments in the presence of either a clinically achievable concentration of 30 μM CBZ or 0.1% DMSO vehicle control. Voltage-clamp studies revealed that

Table 2. Biophysical properties of WT and V810M channels following 30-min preincubation with either 30 μM CBZ or 0.1% DMSO vehicle control.

Na$_v$1.7	Drug	Activation (mV)			Steady-state fast inactivation (mV)			Use dependence (20 Hz)	
		V$_{1/2}$	k	n	V$_{1/2}$	k	n	Percent	n
WT	DMSO	−18.6 ± 0.8	8.2 ± 0.3	15	−87.3 ± 1.3	6.8 ± 0.2	15	78.5% ± 1.5	15
	CBZ	−20.2 ± 1.0	7.8 ± 0.2	12	−89.9 ± 1.5	7.1 ± 0.2	11	70.0% ± 1.7*	12
V810M	DMSO	−20.9 ± 0.5	7.8 ± 0.2	15	−87.8 ± 1.4	6.5 ± 0.2	14	77.1% ± 1.7	14
	CBZ	−21.5 ± 0.8	7.5 ± 0.3	13	−88.1 ± 1.9	6.8 ± 0.2	13	70.7% ± 1.6*	12

Note: CBZ: carbamazepine; DMSO: dimethyl sulfoxide.
*$p < 0.01$ significantly different from DMSO; n represents the number of cells from which recordings were acquired.

CBZ had no detectable effect on activation of either WT or V810M channels (Table 2, Figure 5(a)). Furthermore, steady-state fast inactivation of neither WT nor V810M was affected by CBZ (Table 2). However, both WT and V810M showed a significant increase in use-dependent inhibition in the presence of CBZ (WT: $p = 0.0001$; V810M: $p = 0.002$; Table 2, Figure 5(c)). Taken together, these data suggest that CBZ acts in this patient with the V810M mutation via the classical mechanism of use-dependent inhibition and not by activation modulation as previously described for other gain-of-function Na$_v$1.7 mutations.[18,22,23]

Discussion

We describe here a patient with painful peripheral neuropathy who carries the Na$_v$1.7-V810M variant. This patient presented with clinical symptoms of severe distal pain and responded to treatment with CBZ. Neither the position of the V810M substitution near the C-terminus of the DII/S3 nor the lack of conservation among other Na$_v$ channel isoforms would have suggested that the V810M mutation might be pathogenic, and it was previously classified in genomic databases as a variant of unknown significance. However, the Na$_v$1.7-V810M allele is rare, and V810 is highly conserved in orthologues of Na$_v$1.7 in various mammalian species (Figure 1), which suggested a possible conserved function. Functional testing revealed gain-of-function attributes that the V810M substitution conferred on the channel, and expression of V810M mutant channels in DRG neurons rendered them hyperexcitable. Taken together, these genetic, clinical, and functional assessments are consistent with the designation of this variant as "pathogenic" or "probably pathogenic" based on classification criteria developed for sequence variants in voltage-gated ion channels.[24]

The sensory disturbances in this patient affected all limbs as well as the back, head, and face, although the chest and abdomen were relatively unaffected. Imaging of the entire neuraxis was normal, as was CSF examination, which is consistent with a functional and not necessarily structural pathophysiological mechanism. Interestingly, pain attacks could be provoked by cold or vibratory stimulation, and symptoms improved with warmth. Although the prototypical cases of burning pain in individuals carrying mutations in Na$_v$1.7 report pain attacks triggered by warmth and relieved by cooling, a natural history study of 13 individuals with IEM carrying well-characterized mutations in Na$_v$1.7 identified an individual who reported cold triggers of pain, even when other members of their family who carry the same mutation reported cold-induced relief.[25] It is likely that additional genetic and epigenetic factors contribute to this individual-to-individual variability in the response to environmental triggers among patients carrying mutations in Na$_v$1.7, but these factors are not well understood at this time.

An additional cardiac comorbidity is present in this patient. He carried a rare variant in Na$_v$1.5 (0.02%, ExAC database), which substitutes glycine (G) by glutamic acid (E) at position 615 (G615E) in the Na$_v$1.5 channel. This variant has been previously reported in patients with irritable bowel syndrome (IBS), both with or without cardiac symptoms, and functional testing showed that it confers loss-of-function attributes on the channel (reduced peak current amplitude and depolarizing shift of activation).[26] Although the patient in our study reported cardiac deficits that required placement of a pacemaker, he did not report symptoms of IBS. Carriers of Na$_v$1.5 mutations have not reported somatic pain symptoms; therefore, the G615E mutation was not considered as a contributor to the pain phenotype in this patient.

The V810M allele is rare and is represented in different databases at < 0.02%. V810 is located at the C-terminal end of transmembrane segment 3 in domain II (DII/S3) in Na$_v$1.7 but is not highly conserved among other members of the sodium channel family. A valine at the corresponding position is conserved only in Na$_v$1.1 and Na$_v$1.4, and the equivalent residue is methionine in Na$_v$1.2, Na$_v$1.3, and Na$_v$1.6. However, a valine residue is
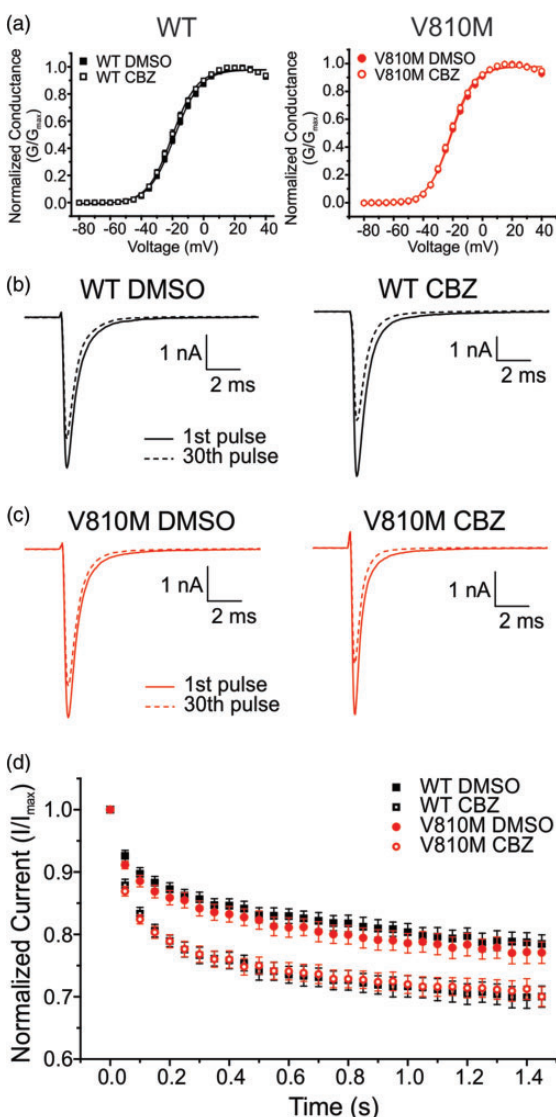
Figure 5. CBZ enhances use-dependent inhibition of V810M and WT channels. (a) Voltage-dependent activation of WT (left; DMSO: solid black squares, $n = 15$; CBZ: open black squares, $n = 12$) and V810M (right; DMSO: solid red circles, $n = 15$; CBZ: open red circles, $n = 13$) channels show no shift in activation following a 30-min preincubation period with 30 µM CBZ as compared to 0.1% DMSO vehicle. Conductance curves were normalized to the maximum conductance value and fit to a Boltzmann equation. (b) Representative traces of use-dependent inhibition of WT channels following a 30-min preincubation period with either 0.1% DMSO vehicle (left) or 30 µM CBZ (right). (c) Representative traces of use-dependent inhibition of V810M channels following a 30-min preincubation period with either 0.1% DMSO vehicle (left) or 30 µM CBZ (right). (d) Use-dependent inhibition curves of WT (DMSO: solid black squares, $n = 15$; CBZ: open black squares, $n = 12$) and V810M (DMSO: solid red circles, $n = 14$; CBZ: open red circles, $n = 12$) channels showing a significant difference between DMSO and CBZ conditions for both channels ($p < 0.05$). Use-dependent inhibition was recorded at 20 Hz and defined as the ratio of peak current of the 30th pulse normalized to peak current of the first pulse. CBZ: carbamazepine; DMSO: dimethyl sulfoxide.

conserved at this position in orthologues of $Na_v1.7$ in mammalian species, except for the rat where it is replaced by isoleucine, which has a branched aliphatic side chain similar to valine (Figure 1). Importantly, functional assessment has shown that V810M substitution confers gain-of-function attributes on the channel. The gain-of-function attributes of the V810M substitution in $Na_v1.7$ are consistent with the view that this residue contributes to the gating of $Na_v1.7$. The presence of methionine at the corresponding position in three voltage-gated sodium channels suggests that the V810M substitution in $Na_v1.7$ may have uncovered an isoform-dependent effect for this residue.

Pain has been linked to hyperexcitability of DRG neurons.[27–30] We assessed the effect of the expression of V810M mutant channels on the excitability of the DRG neurons. MEA recordings have the benefit of assessing the excitability of intact neurons and in this case demonstrated enhanced excitability of DRG neurons expressing the V810M mutant channels. The gain-of-function attributes at the neuronal level included total number of spikes per well, mean firing frequency, and number of active electrodes (Figure 4). Our MEA data supports the pathogenicity of the V810M mutation and provide further evidence for a mechanistic basis for pain in this individual.

Although the patient has carried the mutation from birth, he began to manifest symptoms in his early 40s, and the symptoms increased in severity by the age of 53, with no clear precipitating events. Gain-of-function mutations of $Na_v1.7$ have been identified in patients with adult-onset SFN[14] and in patients with type 2 diabetic neuropathy and pain.[15] Gain-of-function mutations in $Na_v1.8$[31–33] and $Na_v1.9$[34,35] have also been found in patients with adult-onset SFN. In a family with the gain-of-function $Na_v1.7$-G616R mutation, pain developed in the proband in his mid-20s, while his children developed pain before the age of 10.[36] The nature of the compensatory factors that prevent pain prior to this age of onset in our patient, as in these other cases, are unknown, but the phenomenon is well-established.

Based on the patient's successful response to CBZ manifested as reduced frequency and severity of pain attacks, we assessed the mechanism of action of this drug on V810M. CBZ is the first-line treatment for trigeminal neuralgia,[37] and subjects with $Na_v1.7$-related PEPD are generally responsive to treatment with CBZ.[38,39] The responsiveness of these patients to CBZ may be due to the classical effect of this drug as a potent state- and use-dependent blocker of neuronal Na_v channels.[40] Recently, a new mode of action of CBZ as an activation modulator in three IEM mutations in $Na_v1.7$ has been described,[19,22,23] where CBZ acts by depolarizing activation. The observed increase in use-

dependent inhibition by CBZ coupled with a lack of an effect on activation of V810M channels suggest that CBZ produces pain relief in this patient via its classical use-dependent mechanism and not via its novel mode of action as an activation modulator. The favorable response of the patient to treatment with CBZ is also suggestive that the V810M mutation did not alter the high-affinity local anesthetic binding site where CBZ binds.[41] It is important to note that CBZ is known to act on other Na_v channel isoforms, and whether its efficacy in relieving pain in this patient is due to Na_v1.7 modulation, effects on other Na_v channel isoforms, or a combination of the two, cannot be definitively determined.

In summary, we report here the identification of a novel rare variant of Na_v1.7 in a patient with adult-onset pain symptoms. Functional assessment of mutant channels demonstrated that the V810M mutation conferred gain-of-function attributes on the channel and rendered DRG neurons that express the mutant channels hyperexcitable. We also assessed the sensitivity of the channel to a clinically achievable concentration of CBZ. Voltage-clamp recordings showed that CBZ did not depolarize activation of the mutant channel but produced use-dependent inhibition which may have contributed to the pain relief reported by the patient.

ORCID iD

Talia Adi (iD) http://orcid.org/0000-0002-3423-3318

References

1. Tsang A, Von Korff M, Lee S, Alonso J, Karam E, Angermeyer MC, Borges GL, Bromet EJ, Demytteneare K, de Girolamo G, de Graaf R, Gureje O, Lepine JP, Haro JM, Levinson D, Oakley Browne MA, Posada-Villa J, Seedat S and Watanabe M. Common chronic pain conditions in developed and developing countries: gender and age differences and comorbidity with depression-anxiety disorders. *J Pain* 2008; 9: 883–891.
2. Elzahaf RA, Tashani OA, Unsworth BA and Johnson MI. The prevalence of chronic pain with an analysis of countries with a Human Development Index less than 0.9: a systematic review without meta-analysis. *Curr Med Res Opin* 2012; 28: 1221–1229.
3. Finnerup NB, Attal N, Haroutounian S, McNicol E, Baron R, Dworkin RH, Gilron I, Haanpaa M, Hansson P, Jensen TS, Kamerman PR, Lund K, Moore A, Raja SN, Rice AS, Rowbotham M, Sena E, Siddall P, Smith BH and Wallace M. Pharmacotherapy for neuropathic pain in adults: a systematic review and meta-analysis. *Lancet Neurol* 2015; 14: 162–173.
4. Dib-Hajj SD, Yang Y, Black JA and Waxman SG. The Na_v1.7 sodium channel: from molecule to man. *Nat Rev Neurosci* 2013; 14: 49–62.
5. Dib-Hajj SD, Geha P and Waxman SG. Sodium channels in pain disorders: pathophysiology and prospects for treatment. *Pain* 2017; 158 Suppl 1: S97–S107.
6. Cummins TR, Howe JR and Waxman SG. Slow closed-state inactivation: a novel mechanism underlying ramp currents in cells expressing the hNE/PN1 sodium channel. *J Neurosci* 1998; 18: 9607–9619.
7. Waxman SG. Neurobiology: a channel sets the gain on pain. *Nature* 2006; 444: 831–832.
8. Vasylyev DV, Han C, Zhao P, Dib-Hajj S and Waxman SG. Dynamic-clamp analysis of wild-type hNaV1.7 and erythromelalgia mutant channel L858H. *J Neurophysiol* 2014; 111: 1429–1443.
9. Alexandrou AJ, Brown AR, Chapman ML, Estacion M, Turner J, Mis MA, Wilbrey A, Payne EC, Gutteridge A, Cox PJ, Doyle R, Printzenhoff D, Lin Z, Marron BE, West C, Swain NA, Storer RI, Stupple PA, Castle NA, Hounshell JA, Rivara M, Randall A, Dib-Hajj SD, Krafte D, Waxman SG, Patel MK, Butt RP and Stevens EB. Subtype-selective small molecule inhibitors reveal a fundamental role for Nav1.7 in nociceptor electrogenesis, axonal conduction and presynaptic release. *PLoS One* 2016; 11: e0152405.
10. Minett MS, Nassar MA, Clark AK, Passmore G, Dickenson AH, Wang F, Malcangio M and Wood JN. Distinct Nav1.7-dependent pain sensations require different sets of sensory and sympathetic neurons. *Nat Commun* 2012; 3: 791.
11. Gingras J, Smith S, Matson DJ, Johnson D, Nye K, Couture L, Feric E, Yin R, Moyer BD, Peterson ML, Rottman JB, Beiler RJ, Malmberg AB and McDonough

SI. Global Nav1.7 knockout mice recapitulate the phenotype of human congenital indifference to pain. *PLoS One* 2014; 9: e105895.

12. Nassar MA, Stirling LC, Forlani G, Baker MD, Matthews EA, Dickenson AH and Wood JN. Nociceptor-specific gene deletion reveals a major role for Nav1.7 (PN1) in acute and inflammatory pain. *Proc Natl Acad Sci USA* 2004; 101: 12706–12711.

13. Shields SD, Cheng X, Uceyler N, Sommer C, Dib-Hajj SD and Waxman SG. Sodium channel Na$_v$1.7 is essential for lowering heat pain threshold after burn injury. *J Neurosci* 2012; 32: 10819–10832.

14. Faber CG, Hoeijmakers JG, Ahn HS, Cheng X, Han C, Choi JS, Estacion M, Lauria G, Vanhoutte EK, Gerrits MM, Dib-Hajj S, Drenth JP, Waxman SG and Merkies IS. Gain of function Na$_V$1.7 mutations in idiopathic small fiber neuropathy. *Ann Neurol* 2012; 71: 26–39.

15. Blesneac I, Themistocleous AC, Fratter C, Conrad LJ, Ramirez JD, Cox JJ, Tesfaye S, Shillo PR, Rice ASC, Tucker SJ and Bennett DLH. Rare Nav1.7 variants associated with painful diabetic peripheral neuropathy. *Pain* 2017; 159: 469–480.

16. Yang Y, Mis MA, Estacion M, Dib-Hajj SD and Waxman SG. NaV1.7 as a pharmacogenomic target for pain: moving toward precision medicine. *Trends Pharmacol Sci* 2018; 39: 258–275.

17. Cao L, McDonnell A, Nitzsche A, Alexandrou A, Saintot PP, Loucif AJ, Brown AR, Young G, Mis M, Randall A, Waxman SG, Stanley P, Kirby S, Tarabar S, Gutteridge A, Butt R, McKernan RM, Whiting P, Ali Z, Bilsland J and Stevens EB. Pharmacological reversal of a pain phenotype in iPSC-derived sensory neurons and patients with inherited erythromelalgia. *Sci Transl Med* 2016; 8: 335–356.

18. Yang Y, Dib-Hajj SD, Zhang J, Zhang Y, Tyrrell L, Estacion M and Waxman SG. Structural modelling and mutant cycle analysis predict pharmacoresponsiveness of a Na$_v$1.7 mutant channel. *Nat Commun* 2012; 3: 1186.

19. Geha P, Yang Y, Estacion M, Schulman BR, Tokuno H, Apkarian AV, Dib-Hajj SD and Waxman SG. Pharmacotherapy for pain in a family with inherited erythromelalgia guided by genomic analysis and functional profiling. *JAMA Neurol* 2016; 73: 659–667.

20. Dib-Hajj SD, Choi JS, Macala LJ, Tyrrell L, Black JA, Cummins TR and Waxman SG. Transfection of rat or mouse neurons by biolistics or electroporation. *Nat Protoc* 2009; 4: 1118–1126.

21. Yang Y, Huang J, Mis MA, Estacion M, Macala L, Shah P, Schulman BR, Horton DB, Dib-Hajj SD and Waxman SG. Nav1.7-A1632G mutation from a family with inherited erythromelalgia: enhanced firing of dorsal root ganglia neurons evoked by thermal stimuli. *J Neurosci* 2016; 36: 7511–7522.

22. Yang Y, Adi T, Effraim P, Chen L, Dib-Hajj SD and Waxman SG. Reverse pharmacogenomics: carbamazepine normalizes activation and attenuates thermal hyperexcitability of sensory neurons due to Nav1.7 mutation I234T. *Br J Pharmacol* 2018; 175: 2261–2271.

23. Fischer TZ, Gilmore ES, Estacion M, Eastman E, Taylor S, Melanson M, Dib-Hajj SD and Waxman SG. A novel Nav1.7 mutation producing carbamazepine-responsive erythromelalgia. *Ann Neurol* 2009; 65: 733–741.

24. Waxman SG, Merkies IS, Gerrits MM, Dib-Hajj SD, Lauria G, Cox JJ, Wood JN, Woods CG, Drenth JP and Faber CG. Sodium channel genes in pain-related disorders: phenotype-genotype associations and recommendations for clinical use. *Lancet Neurol* 2014; 13: 1152–1160.

25. McDonnell A, Schulman B, Ali Z, Dib-Hajj SD, Brock F, Cobain S, Mainka T, Vollert J, Tarabar S and Waxman SG. Inherited erythromelalgia due to mutations in SCN9A: natural history, clinical phenotype and somatosensory profile. *Brain* 2016; 139: 1052–1065.

26. Beyder A, Mazzone A, Strege PR, Tester DJ, Saito YA, Bernard CE, Enders FT, Ek WE, Schmidt PT, Dlugosz A, Lindberg G, Karling P, Ohlsson B, Gazouli M, Nardone G, Cuomo R, Usai–Satta P, Galeazzi F, Neri M, Portincasa P, Bellini M, Barbara G, Camilleri M, Locke GR, Talley NJ, D'Amato M, Ackerman MJ and Farrugia G. Loss-of-function of the voltage-gated sodium channel NaV1.5 (channelopathies) in patients with irritable bowel syndrome. *Gastroenterology* 2014; 146: 1659–1668.

27. Ochoa J and Torebjork E. Sensations evoked by intraneural microstimulation of C nociceptor fibres in human skin nerves. *J Physiol* 1989; 415: 583–599.

28. Kleggetveit IP, Namer B, Schmidt R, Helas T, Ruckel M, Orstavik K, Schmelz M and Jorum E. High spontaneous activity of C-nociceptors in painful polyneuropathy. *Pain* 2012; 153: 2040–2047.

29. Haroutounian S, Nikolajsen L, Bendtsen TF, Finnerup NB, Kristensen AD, Hasselstrom JB and Jensen TS. Primary afferent input critical for maintaining spontaneous pain in peripheral neuropathy. *Pain* 2014; 155: 1272–1279.

30. Vaso A, Adahan HM, Gjika A, Zahaj S, Zhurda T, Vyshka G and Devor M. Peripheral nervous system origin of phantom limb pain. *Pain* 2014; 155: 1384–1391.

31. Han C, Vasylyev D, Macala LJ, Gerrits MM, Hoeijmakers JG, Bekelaar KJ, Dib-Hajj SD, Faber CG, Merkies IS and Waxman SG. The G1662S NaV1.8 mutation in small fibre neuropathy: impaired inactivation underlying DRG neuron hyperexcitability. *J Neurol Neurosurg Psychiatry* 2014; 85: 499–505.

32. Faber CG, Lauria G, Merkies IS, Cheng X, Han C, Ahn HS, Persson AK, Hoeijmakers JG, Gerrits MM, Pierro T, Lombardi R, Kapetis D, Dib-Hajj SD and Waxman SG. Gain-of-function Nav1.8 mutations in painful neuropathy. *Proc Natl Acad Sci USA* 2012; 109: 19444–19449.

33. Huang J, Yang Y, Zhao P, Gerrits MM, Hoeijmakers JG, Bekelaar K, Merkies IS, Faber CG, Dib-Hajj SD and Waxman SG. Small-fiber neuropathy Nav1.8 mutation shifts activation to hyperpolarized potentials and increases excitability of dorsal root ganglion neurons. *J Neurosci* 2013; 33: 14087–14097.

34. Han C, Yang Y, de Greef BT, Hoeijmakers JG, Gerrits MM, Verhamme C, Qu J, Lauria G, Merkies IS, Faber CG, Dib-Hajj SD and Waxman SG. The domain II S4-S5 linker in Nav1.9: a missense mutation enhances activation, impairs fast inactivation, and produces human painful neuropathy. *Neuromol Med* 2015; 17: 158–169.

35. Huang J, Han C, Estacion M, Vasylyev D, Hoeijmakers JG, Gerrits MM, Tyrrell L, Lauria G, Faber CG, Dib-Hajj SD, Merkies IS and Waxman SG. Gain-of-function mutations in sodium channel Na$_v$1.9 in painful neuropathy. *Brain* 2014; 137: 1627–1642.

36. Choi JS, Cheng X, Foster E, Leffler A, Tyrrell L, Te Morsche RH, Eastman EM, Jansen HJ, Huehne K, Nau C, Dib-Hajj SD, Drenth JP and Waxman SG. Alternative splicing may contribute to time-dependent manifestation of inherited erythromelalgia. *Brain* 2010; 133: 1823–1835.

37. Cruccu G, Bonamico LH and Zakrzewska JM. Cranial neuralgias. *Handb Clin Neurol* 2010; 97: 663–678.

38. Fertleman CR, Baker MD, Parker KA, Moffatt S, Elmslie FV, Abrahamsen B, Ostman J, Klugbauer N, Wood JN, Gardiner RM and Rees M. SCN9A mutations in paroxysmal extreme pain disorder: allelic variants underlie distinct channel defects and phenotypes. *Neuron* 2006; 52: 767–774.

39. Fertleman CR, Ferrie CD, Aicardi J, Bednarek NA, Eeg-Olofsson O, Elmslie FV, Griesemer DA, Goutieres F, Kirkpatrick M, Malmros IN, Pollitzer M, Rossiter M, Roulet-Perez E, Schubert R, Smith VV, Testard H, Wong V and Stephenson JB. Paroxysmal extreme pain disorder (previously familial rectal pain syndrome). *Neurology* 2007; 69: 586–595.

40. Thomas AM and Atkinson TJ. Old friends with new faces: are sodium channel blockers the future of adjunct pain medication management? *J Pain* 2018; 19: 1–9.

41. Fozzard HA, Sheets MF and Hanck DA. The sodium channel as a target for local anesthetic drugs. *Front Pharmacol* 2011; 2: 68.